STM JOURNALS

Journal of
Polymer & Composites

ISSN: 2321-2810 (Online)
ISSN: 2321-8525 (Print)
Volume 13, Special Issue 5, 2025
DOI (Journal): 10.37591/JoPC

https://journals.stmjournals.com/jopc

Research JoPC

Thermal Management of Different Composites Materials Using a Convergent and Straight Vortex Tube

Ravi Kant Singh[1,*], Pankaj Dashore[2], Rachana Dashore[3], Vandana Purushottam Chitodkar[4], Shraddha Bhausaheb Navle[5], Supriyatai Kailashrao Ahire[6], Rajeev Kumar[7], Subhash Gautam[8]

Abstract

The present study focuses on an in-depth and meticulous exploration into the intricate realm of thermal management in three distinct yet widely utilized composite materials—namely, Liquid Crystal Polymer (LCP) Composites, Glass Fiber Reinforced Polymers (GFRPs), and Aramid Fiber Composites (Kevlar). This investigation employs an innovative counter-flow vortex tube system, meticulously analyzing and comparing the thermal efficiency of these materials under different intake configurations. Specifically, two distinct geometrical intake designs—a straight tube section and an advanced convergent tube section—are systematically scrutinized to unravel their impact on flow behavior and energy separation dynamics. A vast array of critical physical and flow parameters are methodically explored, including the influence of convergent angles (θ), intake pressures, cold mass fraction, and flow separation dynamics. Using the powerful ANSYS FLUENT simulation software, air is employed as the working fluid to simulate complex thermal interactions within the vortex tube system. Furthermore, an extensive analysis is performed on essential performance parameters, such as the hot temperature gradient (ΔTh), cold temperature gradient (ΔTc), intake pressure variations, and overall thermal distribution to optimize the vortex tube's cooling efficiency. The research findings of this investigation reveal that Aramid Fiber Composites (Kevlar) exhibit significantly superior thermal sustainability compared to Liquid Crystal Polymer (LCP) Composites and Glass Fiber Reinforced Polymers (GFRPs), particularly when subjected to a convergent vortex tube with an optimized 5-degree angle. This study not only enhances the fundamental understanding of composite material performance under permissible thermal limits but also paves the way for next-generation cooling strategies in aerospace, automotive, and high-performance engineering applications.

***Author for Correspondence**
Ravi Kant Singh

[1,7,8]Assistant Professor, Department of Mechanical Engineering, Sandip Institute of Technology and Research Centre, Nashik, Maharashtra, India
[2]Professor, Department of SOCSE, Sandip University, Nashik, Maharashtra, India
[3]Professor, Department of Master of Business Administration, Sandip Institute of Technology and Research Centre, Nashik, Maharashtra, India
[4]Assistant Professor, Department of Applied Science, Sandip Polytechnic, Nashik, Maharashtra, India
[5,6]Assistant Professor, Department of Engineering Sciences and Humanities, Sandip Institute of Technology and Research Centre, Nashik, Maharashtra, India

Received Date: January 16, 2025
Accepted Date: March 18, 2025
Published Date: July 11, 2025

Citation: Ravi Kant Singh, Pankaj Dashore, Rachana Dashore, Vandana Purushottam Chitodkar, Shraddha Bhausaheb Navle, Supriyatai Kailashrao Ahire, Rajeev Kumar, Subhash Gautam. Thermal Management of Different Composites Materials Using a Convergent and Straight Vortex Tube. Journal of Polymer & Composites. 2025; 13(Special Issue 5): S252–S266p.

Keywords: Liquid crystal polymer (LCP) composites, glass fiber reinforced polymers (GFRPs), aramid fiber composites (kevlar), standard k-ε model, convergent vortex tube, ANSYS FLUENT

INTRODUCTION

Composite materials are a class of engineered materials designed to achieve superior performance by combining two or more distinct components with complementary properties. Typically, composites consist of a matrix phase, which acts as a binder and provides shape and load transfer, and a reinforcement phase, which contributes strength, stiffness, and durability. The synergistic interaction between these phases enables composites to exhibit exceptional chemical, thermal, and mechanical properties.

Composites have become indispensable in various industries, including aerospace, automotive, electronics, and energy, due to their unique advantages such as high strength-to-weight ratio, corrosion resistance, and the ability to tailor properties for specific applications. Advances in composite materials, such as the development of fiber-reinforced polymers, ceramic matrix composites, and metal matrix composites, have further expanded their applications in high-performance and extreme environments.

Huang et al. [1] studied the use of flexible form phase change material for the thermal managements system in the Li-ion battery. They prepared a composite material, with supporting material as styrene butadiene styrene, expanded graphite as thermal conductivity enhancer, and paraffin as a phase change material. Chen et al. [2] studied a hybrid battery thermal managements system with composite PCM containing expanded graphite. They observed that there was 33.3% drop in the power consumption with same load with this hybrid model of thermal managements system.

The vortex tube (VT) is a highly efficient mechanical device because it has no moving parts, resulting in minimal wear and tear. Ranque [3], found accidently the vortex tube while examining the flow in cyclone separators. Since its discovery, improvements in VT performance have been ongoing because of its effective chilling and low maintenance. Skye et al. [4] studied the performance of the VT by experimenting with various mass fractions and inlet pressure, both with experiments and through simulations. They found that as inlet pressure increases, the cold temperature decreases.

The effect of VT's convergent geometry on the flow pattern was explored by Seibold and Weigand [5]. Delayed Detached Eddy Simulations rule was employed, with a swirl number of 5.3 and Reynolds number of 10,000. Celik et al. [6] examine the effect of connecting a vortex tube to a diesel engine at temperatures (-30°C, 0°C, 40°C, and 50°C) for cold start. The positive effects on exhaust emissions, including carbon monoxide (CO), hydrocarbons (HC), nitrogen oxides (NOx), and particulate matter (PM) were also measured. Vitovsky [7] experimentally explained an energy separation in a VT by incorporating a vortex generator inside the VT. He suggested that this modification enhances thermal separation in the VT. Mirjalili et al. [8] has performed the numerical studied on the VT in transient condition. They performed the investigation on the mass fraction range of 0.22 to 0.82 and at various tube length ratio. The result concludes that there is no decomposition of vortices close to cold exit. Li et al. [9] performed a basic flow analysis by separating the vortex tube into six parts. They proposed an equation for the axial velocity component, developed a method for calculating reversed flow, and provided descriptions based on different partitions.

However, the impact of different boundary condition treatment for the VT has been analysed by Dyck et al. [10]. The 3D VT has been considered for simulating the flow for different turbulent model Scale-Adaptive-Simulation SST, k – ω, k – ω and, k – ε. Rajpal et al. [11] has comes up with a right-angled ribbed geometry vortex tube and compared this model with a conventional vortex tube for thermal performance. They advocate that the right-angled ribbed geometry model VT performance better than conventional VT under same working condition. Singh et al. [12-21] explained the various parameters effects on the vortex tube performance.

This study aims to explore the properties, applications, and challenges associated with composite materials, focusing on their behavior under thermal conditions using vortex tube and their role in modern engineering systems. By understanding the fundamental mechanisms governing composite performance, the research seeks to contribute to the development of more efficient and reliable composite solutions for critical applications. So, the present study deal with the thermal performance of composite material namely Liquid Crystal Polymer (LCP) Composites, Glass Fiber Reinforced Polymers (GFRPs), and Aramid Fiber Composites (Kevlar) using a counter-flow vortex tube, examining models with different intake configurations: straight tube section, and convergent tube section ANSYS Fluent software.

MATHEMATICAL MODELLING

The partial differential equations used for solving the complex flow simulation inside the vortex tube are as follows

Continuity Equation:

$$\frac{\partial}{\partial x_i}\left(\rho u_i\right)=0 \tag{1}$$

Momentum Balance Equation:

$$\frac{\partial}{\partial x_i}(\rho u_i u_j)=-\frac{\partial P}{\partial x_i}+\frac{\partial}{\partial x_j}\left[\mu\left(\frac{\partial u_i}{\partial x_i}+\frac{\partial u_j}{\partial x_i}-\frac{2}{3}\delta_{ij}\frac{\partial u_k}{\partial x_k}\right)\right]+\frac{\partial}{\partial x_i}\left(\overline{-\rho u_i' u_j'}\right) \tag{2}$$

Energy Balance Equation:

$$\frac{\partial}{\partial x_i}\left[u_i(\rho E+P)\right]=\frac{\partial}{\partial x_j}\left[\left(k_e+\frac{c_p\mu_t}{\mathrm{Pr}_t}\right)\frac{\partial T}{\partial x_j}+u_i(\tau_{ij})_{eff}\right]+S_h \tag{3}$$

$$(\tau_{ij})_{eff}=\mu_{eff}\left(\frac{\partial u_j}{\partial x_i}+\frac{\partial u_i}{\partial x_j}\right)-\frac{2}{3}\mu_{eff}\frac{\partial u_k}{\partial x_k}\delta_{ij} \tag{4}$$

Ideal gas equation:

$$P=\rho R T_s \tag{5}$$

Meshing, Computational Domain and Model Solver

Numerical simulations were performed using ANSYS FLUENT 17.1 software. The governing equation has been solved with pressure based implicit solver. The momentum equation and convective term has been resolved by a second order scheme.

The schematic view of the test model has been shown in Figure. 1. The grids for the 3D model of VT with straight and convergent main tube models are presented in Figure. 2. Figure. 3 illustrates that grid density has a notable impact on stability and convergence properties. As shown in the Figure, the working fluid temperature decreases with an increase in the number of grid cells. However, beyond 305,000 grid cells, the change in cold exit temperature becomes negligible. Thus, further increasing the grid cell count would be unnecessary, adding computational load and increasing processing time. Consequently, 310,850 grid cells were selected for further simulations in this study.

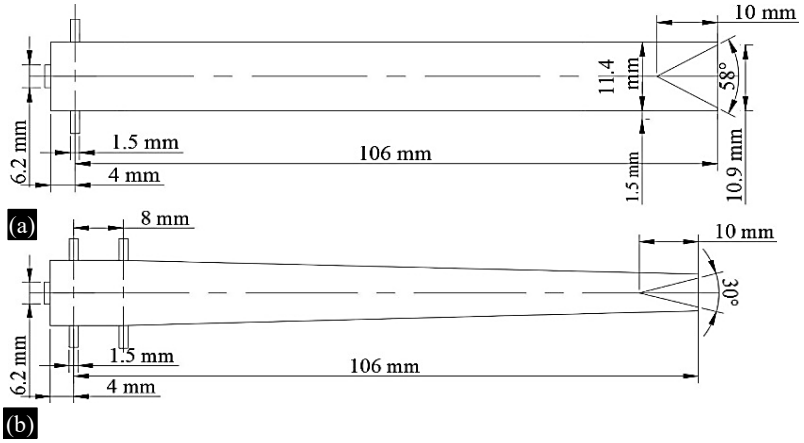

Figure 1. Schematic view of the (a) VT with single section, (b) dual intake section convergent vortex tube.

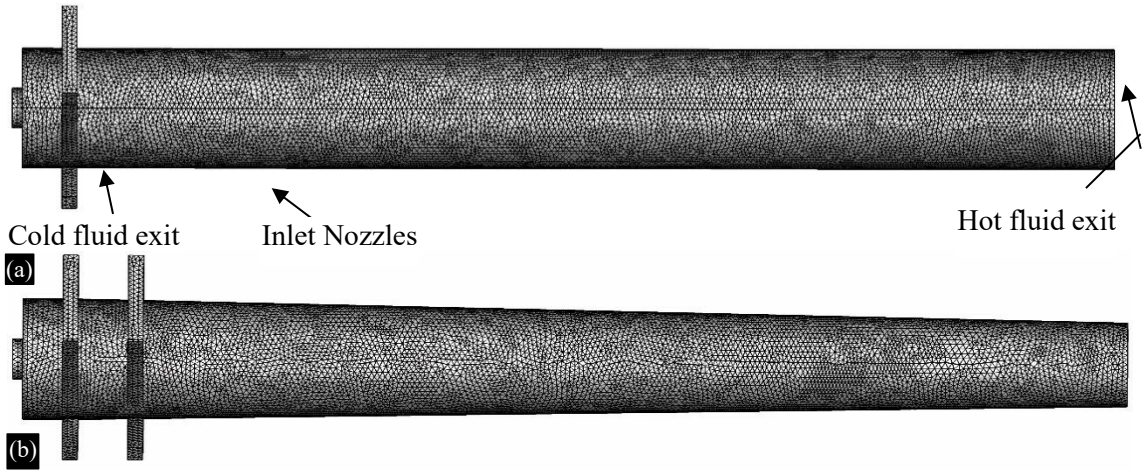

Figure 2. Uniform unstructured mesh of VT with (a) straight main tube, (b) dual inlet section with convergent tube.

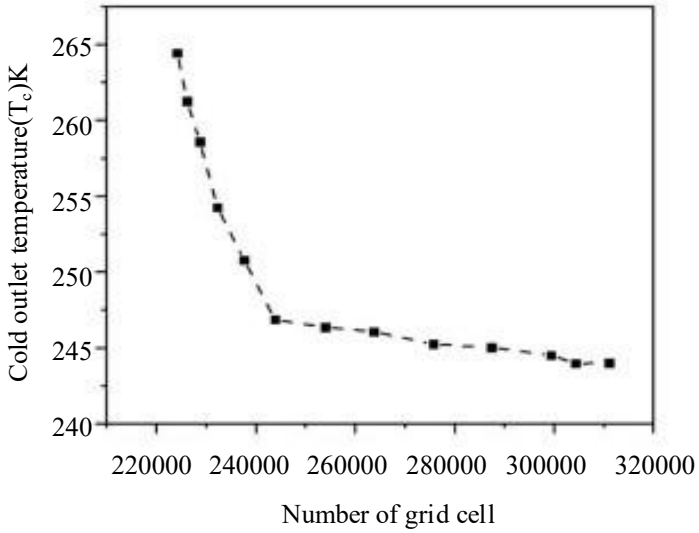

Figure 3. Grid independence evaluation.

Validation

Using FLUENT software, the Navier-Stokes equation related to the conventional k-ε turbulence model has been generated and solved. The present single chamber VT exploration has been validated by comparison with Thakare et al. [22] CFD and experimental results. Figure. 4 shows the change in cold temperature with μ_c. As shown in Figure. 4, the ΔT_c values obtained using the present 3D model are in agreement with CFD and experimental results by Thakare et al. [22]. This proves that the appropriate approach used to model the present investigation was used.

Figure. 4 shows that when μc rises, ΔT_c rises as well, reaches its maximum, and then tends to decrease. 6.5% is the mean variation for the total μ_c. The study's conclusions align with Thakare's [22].

RESULTS AND DISCUSSION

The study has been perform using CFD simulation to examine the thermal analysis, temperature distribution, and velocity of flow in both the type of VT, namely straight, and convergent dual inlet section VT. The VT performance for different operating conditions such as cold mass fraction, intake pressure variation, and convergent angle variation is also analyzed. The hot temperature difference (ΔT_h), cold temperature difference (ΔT_c), and pressure variation in all three models.

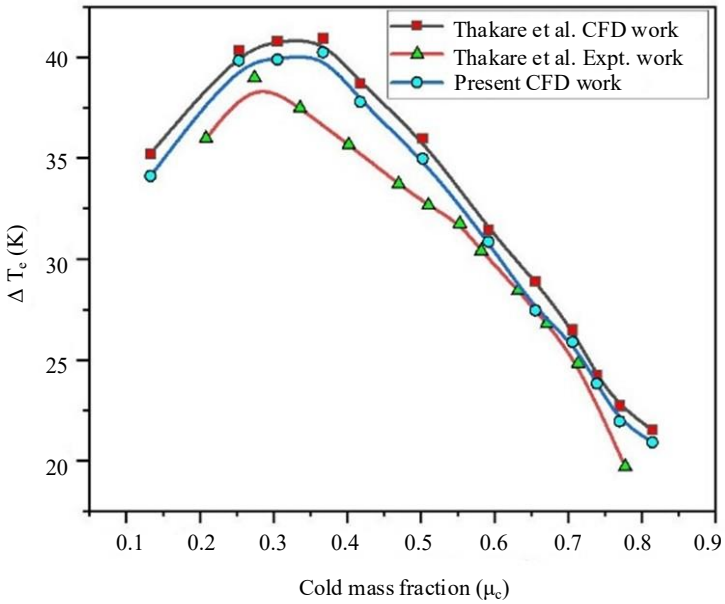

Figure 4. Comparison of present study with previous outcomes by noting the variation in ΔT_c with μ_c

Flow Pattern and Velocity Components

The velocity streamlines path of fluid particle inside the VT for different shapes, as presented in Figure. 5(a) to (c), respectively. It is noted in all the cases of Figure. 5 that the maximum velocity zone lies nearby the intake of the VT, and there is gradual decrement in velocity when the flow advances in the direction of hot outlet due to increase in the pressure due to throttle valve. The velocity becomes zero at the stagnation point, and flow reversal occurs thereafter. Figure. 5 also shows that there exist two flows inside the vortex tube, one near the periphery, which is hotter fluid, that exits in the direction of flow, and another is colder fluid at the core, which flows opposite to the direction of inlet fluid and obtains through the cold exit of VT. The KE of peripheral flow is responsible for temperature increase nearby the hot end, while pressure expansion and the transfer of angular momentum are mostly responsible for the temperature reduction towards the cold exit.

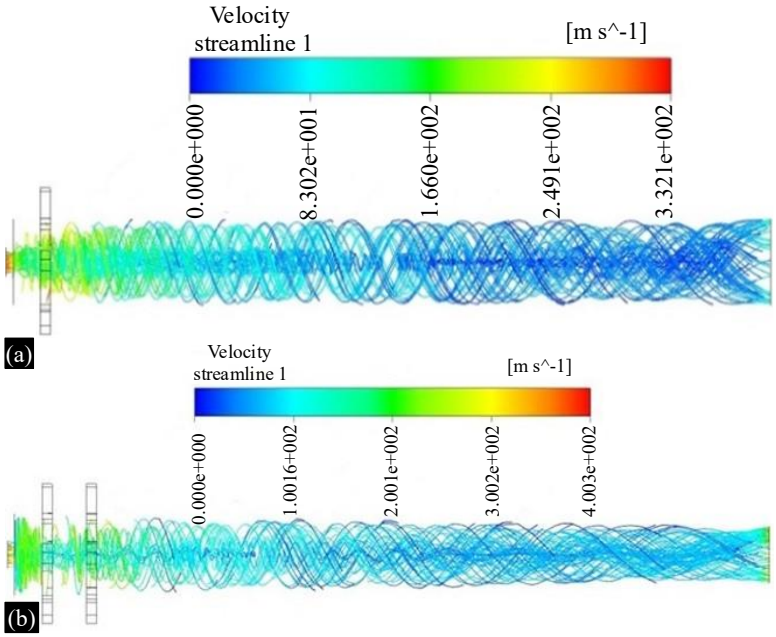

Figure 5. Streamlines formation by the fluid in VT for (a) single intake section, (b) dual intake section with convergent main tube.

Temperature Distribution

The total temperature variation with the radius of the VT at different convergent angles from 1^0 to 5^0 at Z/L= 0.1, Z/L= 0.5, and Z/L= 0.8 has been depicted in Figure. 6 (a) to (c). It can be noted from Figure. 6 that as we move from core (R=0) to periphery (R=5.57mm) in the VT, the total temperature increases gradually from a minimum at the core and maximum at the periphery. It follows a similar trend for all longitudinal positions in the VT for the entire convergent angle considered. As the angle of convergent increases, the total temperature at cold exit decreases, which is noted in all three cases due to increases of pressure at the throttle near the hot exit, which assists the temperature separation phenomenon. Furthermore, as moving from inlet to hot exit along the direction of peripheral fluid flow from Z/L= 0.1 to 0.8, the total temperature magnitude increases from colder region (Z/L= 0.1) to the hotter region (Z/L= 0.8), which can be supported by Figure. 7 for all the cases considered.

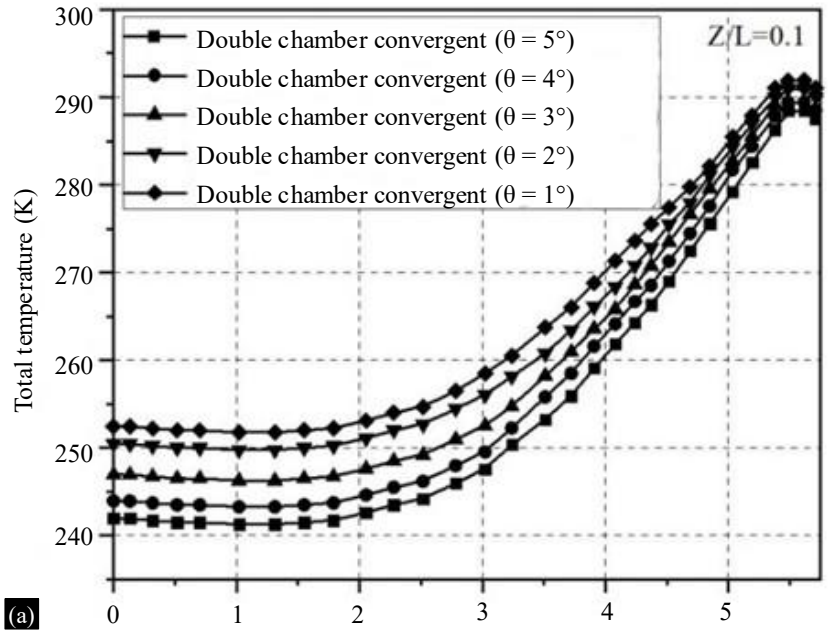

(a)

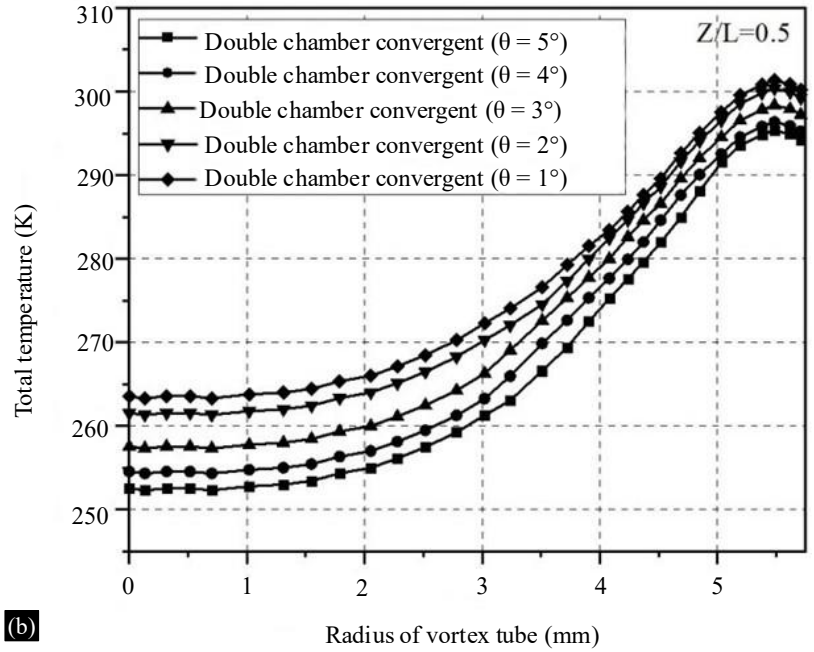

(b)

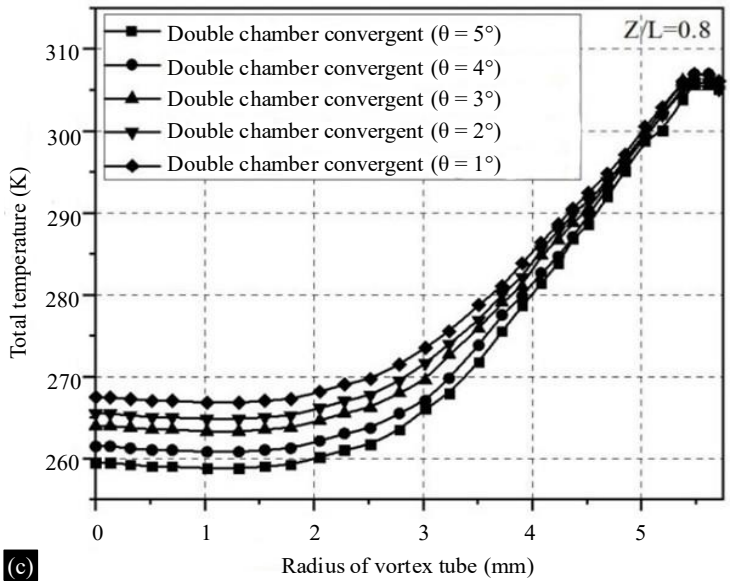

Figure 6. Total temperature variation with radius of vortex tube for different convergent angle for a dual section convergent VT at Z/L=0.1, 0.5, and 0.8.

The temperature contour distribution for a VT of different shapes for intake pressure of 0.6MPa is depicted in Figure. 7 (a) to (c). It is observed from Figure. 7 (a) and (b) that the minimum temperature through cold exit decreases from 264.14 K to 244.34 K as second intake section is introduced, because as the intake section increases, the rate of flow of fluid increases, leading to the higher molecular momentum transfer between the core and peripheral fluid, which further decreases the temperature of intake fluid at cold outlet. The temperature through the cold exit for dual intake convergent vortex tube from Figure. 7 (c) is minimum (239.34 K) among all the types of VT considered for study under the same working condition. The convergence of the main tube of VT increases pressure at the throttle value near the hot exit, which supports the flow separation between core and peripheral fluid flow, but beyond convergent angle of 5^0 the intermingling of the core and peripheral fluid increases, which gradually increases the temperature of cold fluid beyond the convergent angle of 5^0. So, for a better result, the convergent angle was kept between 2^0 to 5^0.

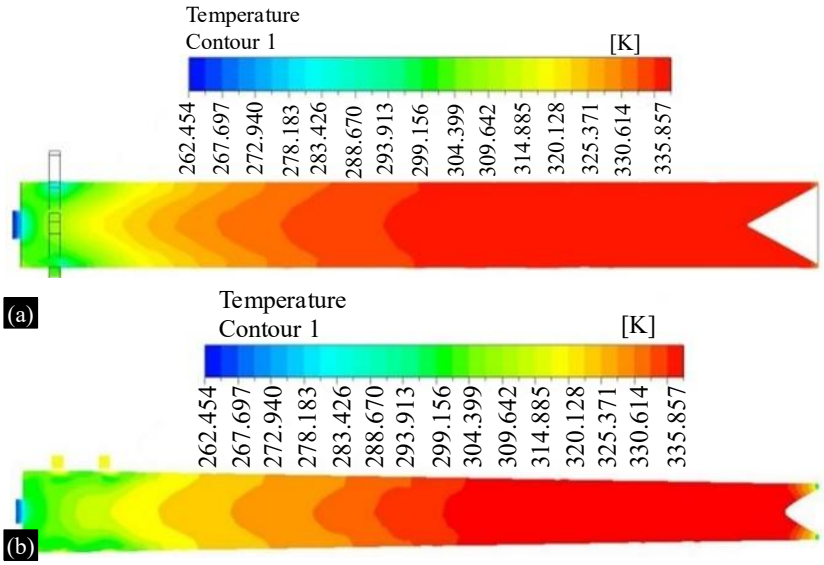

Figure 7. Temperature contour variation of (a) single intake section, (b) dual intake section with the convergent main tube

Thermal Pattern Study

Figure. 8 (a) to (d) depicts ΔT_c versus β variation at Pin = 0.3 to 0.6 MPa respectively. The study was performed for a straight and dual intake section convergent VT with convergent angles 1^0 to 5^0 at different intake pressure. As the value of pressure loss (β) increases, the value of (ΔT_c) attains maxima at β=0.62 and then decreases. The trend of (ΔT_c) with β is common for all the cases and at all intake pressure considered. The maximum value of ΔT_c is 31.2 K at β = 0.64 and Pin = 0.6 MPa for 5^0 convergent angle vortex tube.

Figure. 9(a) to (d) depicts the effect of pressure loss ratio (β) on the ΔT_h for different shapes of VT at different intake pressure P=0.3MPa, 0.4MPa, 0.5MPa, and 0.6MPa. In all cases of Fig. 9, ΔT_h value increases as β increases. This trend is common in all cases. As the pressure at inlet shows increment from 0.3MPa to 0.6MPa, the value of ΔT_h increases. Figure. 9(c) and 9(d) depict that there is not much difference in the value of the ΔT_h after P=0.5 MPa. The value of the ΔT_h is maximum for a dual section vortex tube with a convergent angle of 5^0 and intake pressure of P=0.6MPa, which is 55.4 K.

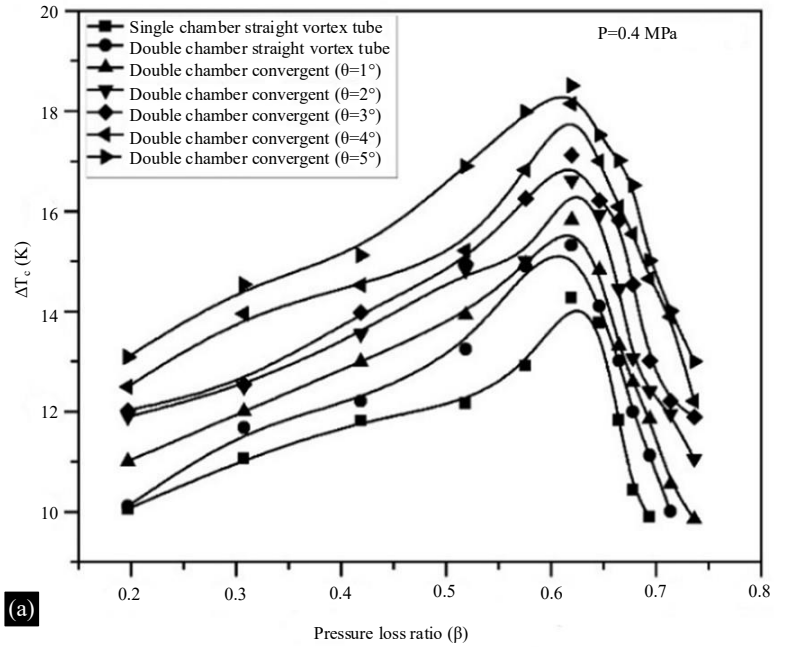

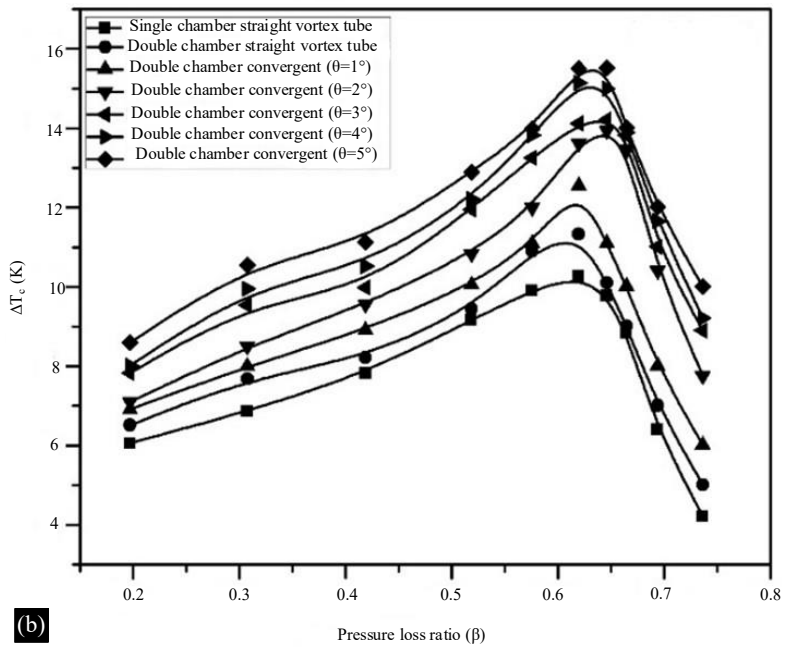

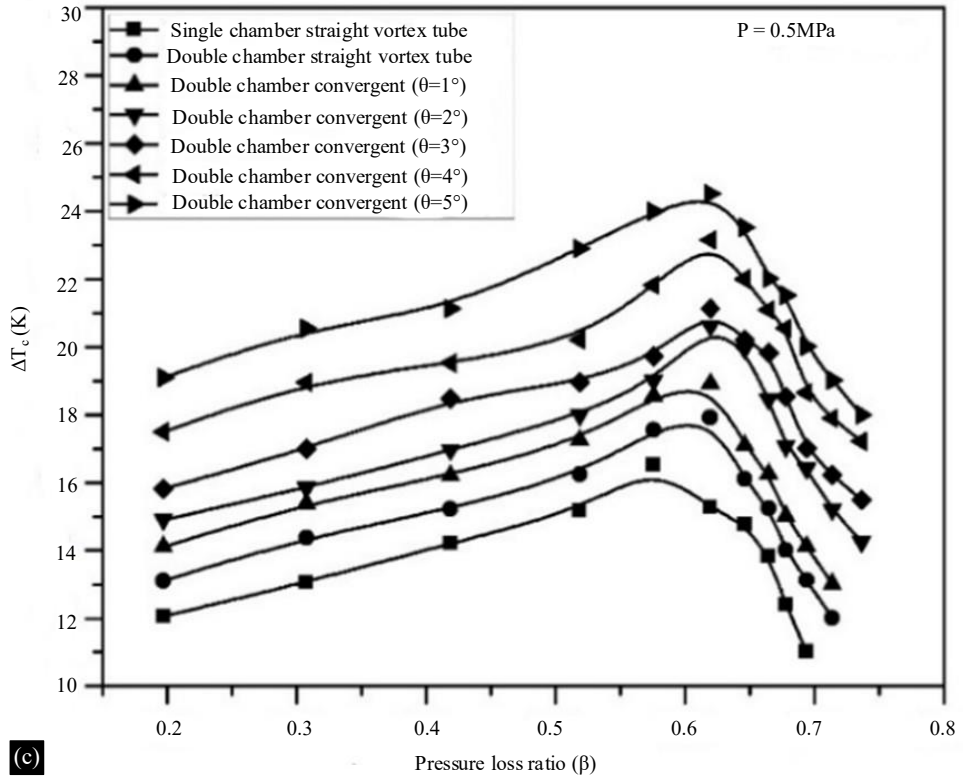

Figure 8. Variation of ΔT_c with β for different VT shapes at intake pressure (a) P=0.3MPa, (b) P=0.4MPa, (c) P=0.5MPa, and (d) P=0.6MPa

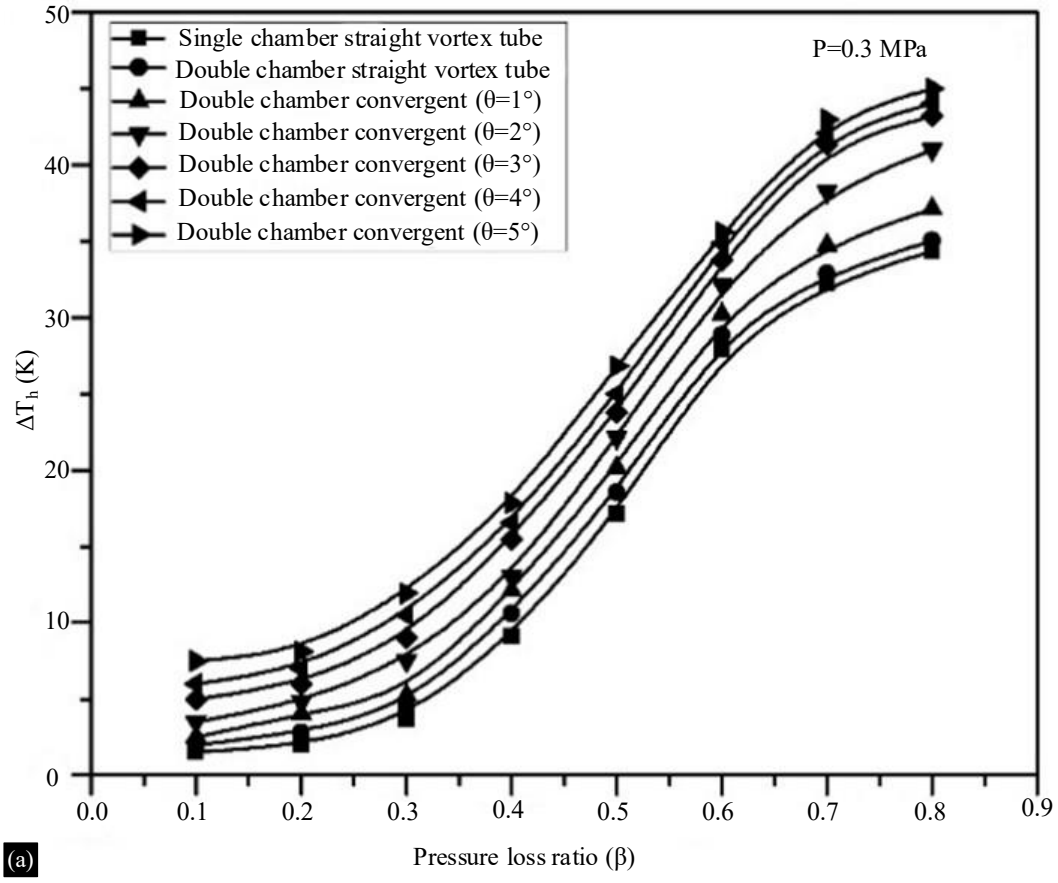

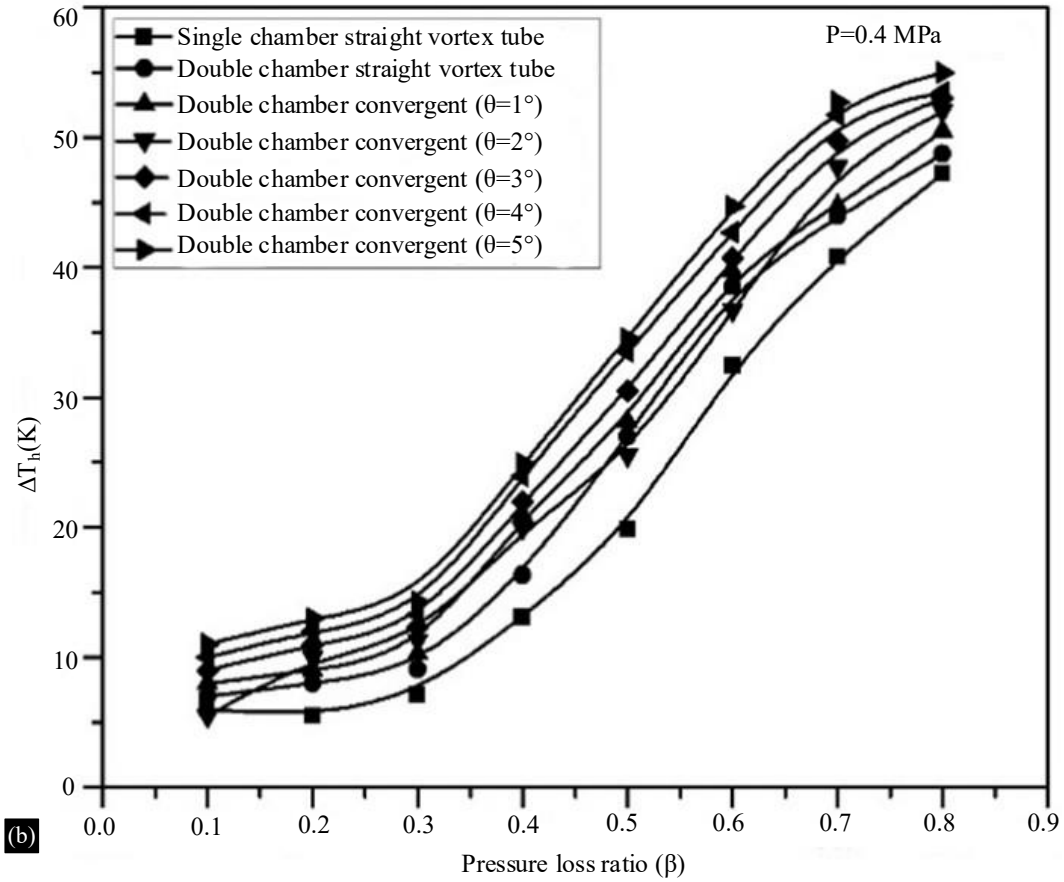

(b)

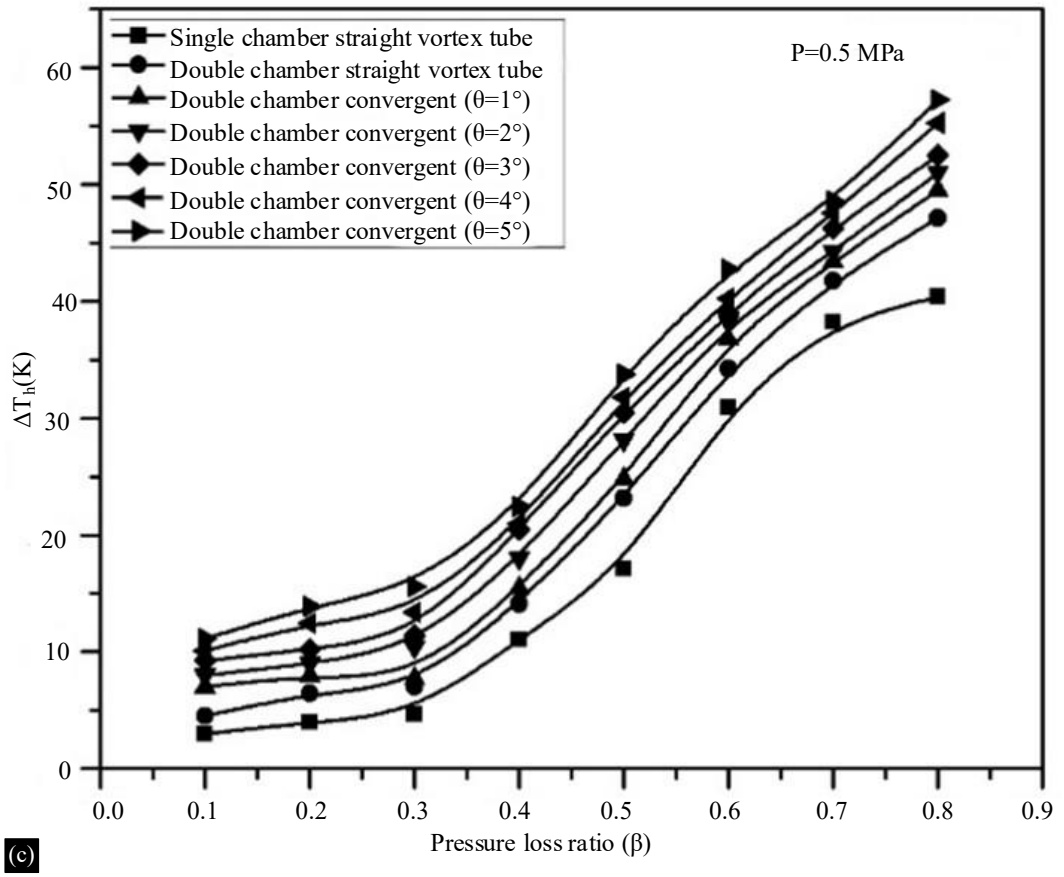

(c)

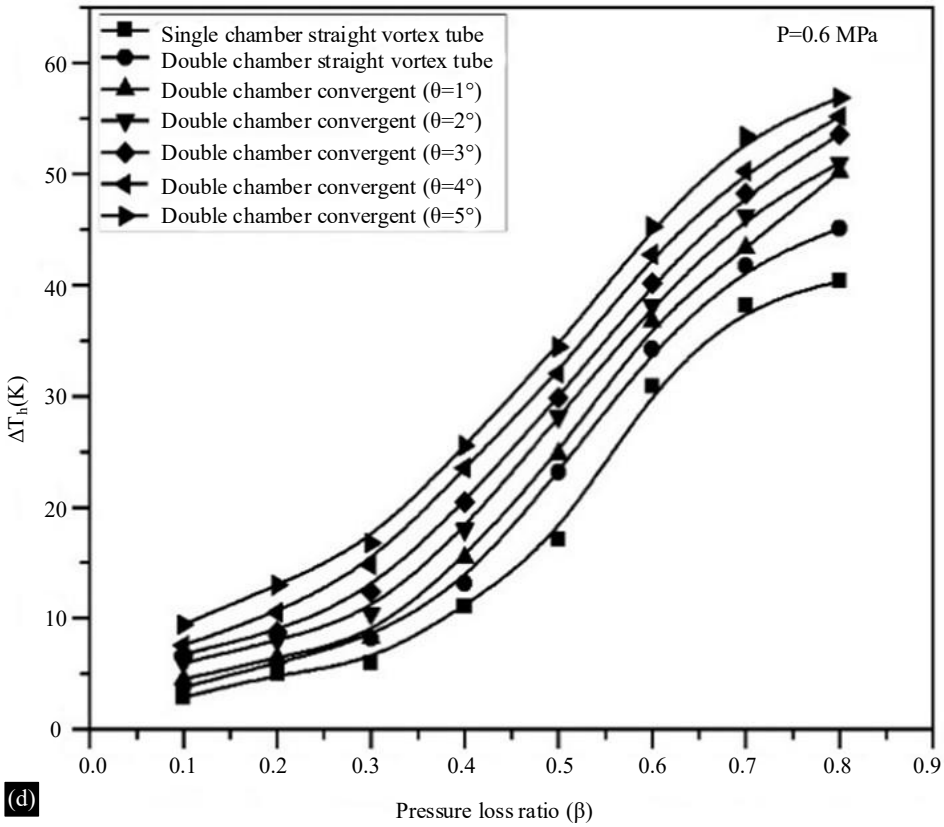

Figure 9. Variation of ΔT_h with β for different VT shapes at different intake pressure (a) P=0.3MPa, (b) P=0.4MPa, (c) P=0.5MPa, and (d) P=0.6MPa

Coefficient of Performance

The cooling impact to the needed work rate is the coefficient of performance (COP)

$$COP = \frac{Q_c}{W} = \frac{\mu C_p \Delta T_c}{\frac{\gamma}{\gamma - 1} RT_{in}\left[\left(\frac{P_{in}}{P_{atm}}\right)^{(\gamma-1)/\gamma} - 1\right]} \quad (6)$$

The external work, specific heat, refrigeration effect, and gas constant, are represented by the letters W, C_p, Q_c, and R. Fig. 10 shows that for all convergent angles taken into consideration, the COP increases as mass fraction rises up to 0.7 and thereafter falls. It is at its peak for the vortex tube with a dual intake section with 5^0 convergent angles. The value of ΔT_c decreases and increases as μ_c rises, rattle the phenomena of temperature separation. Thakare [20] and Skye [2] have noted comparable patterns for COP.

The comparison showing the effect of temperature on thermal management properties for Liquid Crystal Polymer (LCP) Composites, Glass Fiber Reinforced Polymers (GFRPs), and Aramid Fiber Composites (Kevlar) in Table 1.

The graph of Figure 11 illustrates the relationship between temperature and performance for the three composite materials namely LCP Composites (Blue Curve): Performance remains high up to ~280°C (near Glass Transition Temperature (T_g)). A rapid decline is observed after T_g, with performance significantly dropping above 300°C. GFRP (Green Curve): Performance declines steadily up to ~150°C. A more noticeable drop occurs between 150°C and 200°C (near T_g), with severe performance loss beyond 200°C. Aramid Fiber Composites (Kevlar, Red Curve): Performance remains stable up to ~300°C. A rapid decline starts near 300°C due to fiber degradation, with substantial performance loss above 320°C.

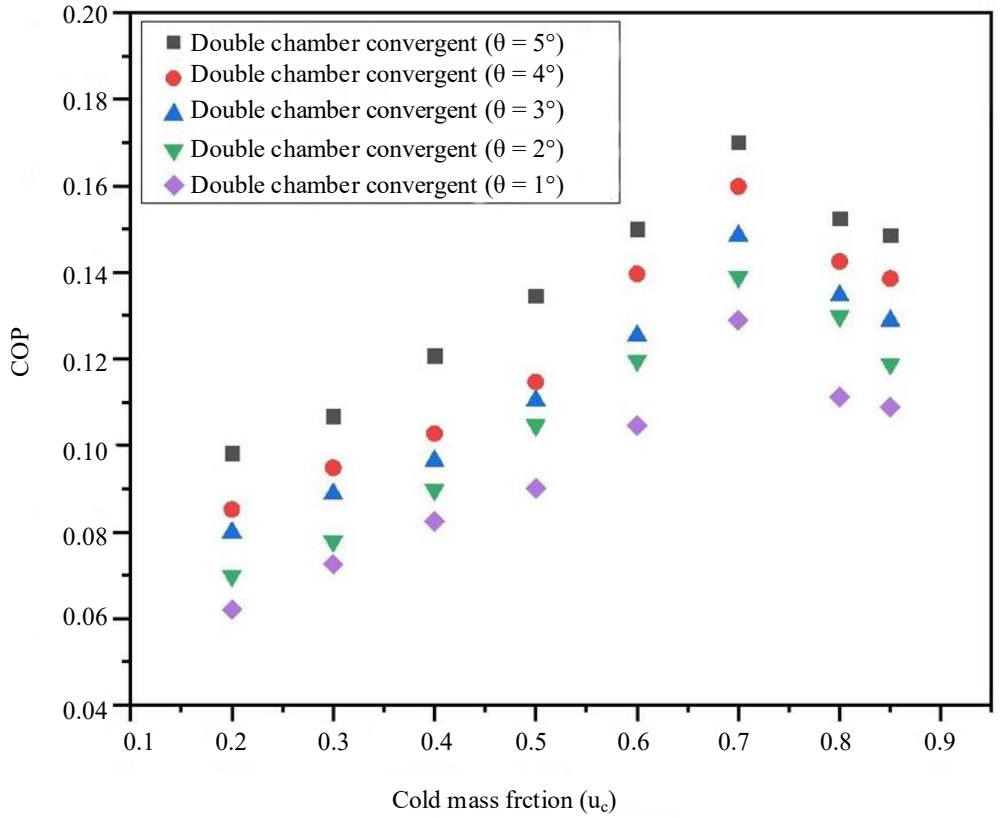

Figure 10. Coefficient of performance variation for dual intake section with cold mass fraction for various convergent angle.

Table 1. Details of Material studied in the present study.

Material	Thermal stability	Glass transition temperature (Tg)	Thermal conductivity	Effect of high temperature	Applications
Liquid Crystal Polymer (LCP) Composites	High thermal stability; retains properties up to ~300°C	~280°C–300°C	~0.2–0.4 W/mK (pure LCP); higher when filled	- Mechanical stability reduces above Tg- Microcracking under thermal cycling- Reduced toughness at extreme temperatures	Connectors, miniature ECU enclosures, EMI shielding
Glass Fiber Reinforced Polymers (GFRPs)	Moderate thermal stability; matrix limits performance	~150°C–200°C	~0.3–0.4 W/mK (fiber)	- Polymer matrix degrades above Tg - Glass fibers remain stable, but matrix softens- Debonding between matrix and fibers	Structural enclosures, industrial ECU housings
Aramid Fiber Composites (Kevlar)	Good stability up to moderate temperatures (~300°C)	~300°C	~0.04 W/mK (fiber)	- Fiber degradation above 300°C- Becomes brittle and loses tensile strength- Not ideal for sustained high-temperature environments	Vibration damping, ballistic protection, housings

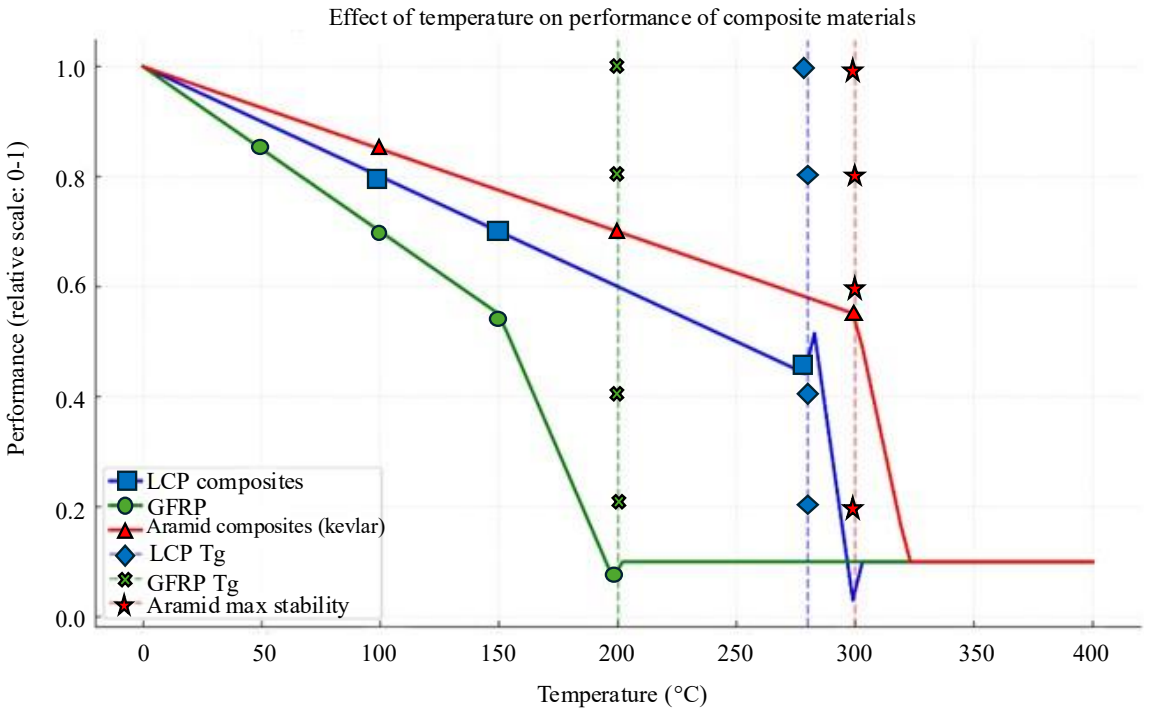

Figure 11. Effect of temperature on performance of composite materials.

CONCLUSIONS

This study highlights the thermal performance characteristics of three widely used composite materials—Liquid Crystal Polymer (LCP) Composites, Glass Fiber Reinforced Polymers (GFRPs), and Aramid Fiber Composites (Kevlar)—and their behavior under varying temperature conditions. The results emphasize the critical role of temperature management in maintaining the structural and functional integrity of these materials.

a. LCP composites demonstrated superior thermal stability, maintaining performance up to their high glass transition temperature (~280°C). This makes them suitable for applications requiring both mechanical strength and efficient thermal management in elevated temperature environments, such as electronic control units (ECUs). GFRPs, while exhibiting moderate thermal resistance with a glass transition temperature of ~200°C, showed significant performance degradation beyond this threshold due to polymer matrix softening. This limits their utility in high-temperature applications but positions them as cost-effective solutions for moderate thermal conditions. Aramid composites (Kevlar), known for their exceptional mechanical properties and stability up to ~300°C, begin to lose performance near their degradation temperature, restricting their use in sustained high-temperature environments.

b. The study underlines the importance of selecting composite materials based on their thermal behavior, particularly in high-performance applications like aerospace, automotive, and electronics. This research reinforces the understanding that thermal management remains a critical parameter for optimizing the performance and longevity of composite materials in high-temperature applications.

c. The impact of intake pressure of fluid on the hot and cold temperature gradient is significant. From Fig. 8 and 9, as the intake pressure increases the value of ΔT_c increases and ΔT_h increases. It is more convincing for the vortex tube with dual intake section having a convergent main tube. It is highest for the convergent angle of 5^0. So, VT with 5^0 convergent angle and dual intake is suitable for the use of thermal management system for maintaining the temperature of composite materials under there permissible limit.

Declaration of Interest

The authors declare that they have no conflicts of interest related to this article.

Acknowledgement

The author acknowledges the support and effort made by all the co-authors and special acknowledgment to department of mechanical engineering NIT Durgapur for supporting with the simulation part of the present study.

REFERENCES

1. Huang Q, Li X, Zhang G, Deng J and Wang C. Thermal management of Lithium-ion battery pack through the application of flexible form-stable composite phase change materials. Applied Thermal Engineering, 2021; 183, p.116151. (JOURNAL)
2. Chen X, Zhou F, Yang W, Gui Y and Zhang Y. A hybrid thermal management system with liquid cooling and composite phase change materials containing various expanded graphite contents for cylindrical lithium-ion batteries. Applied Thermal Engineering. 2022; 200, p.117702. (JOURNAL)
3. Ranque GJ, GIRATION DES FLUIDES SARL method and apparatus for obtaining from alpha fluid under pressure two currents of fluids at different temperatures. 1934; 1,952,281.(U.S. Patent)
4. Skye HM, Nellis GF, Klein SA. Comparison of CFD analysis to empirical data in a commercial vortex tube. International journal of refrigeration. 2006; 29(1):71–80. (JOURNAL)
5. Seibold F and Weigand B. Numerical analysis of the flow pattern in convergent vortex tubes for cyclone cooling applications. International Journal of Heat and Fluid Flow. 2021; 90, p.108806. (JOURNAL)
6. Celik A, Yilmaz M, Kaya M and Karagoz S. The experimental investigation and thermodynamic analysis of vortex tubes. Heat and Mass Transfer. 2017; 53, pp.395-405. (JOURNAL)
7. Vitovsky OV. Experimental study of energy separation in a Ranque-Hilsch tube with a screw vortex generator. International Journal of Refrigeration. 2021; 126, pp.272-279. (JOURNAL)
8. Mirjalili M and Ghorbanian K. Numerical investigation of transient thermo-fluid processes in a Ranque-Hilsch vortex tube. International Journal of Refrigeration. 2021 131, pp.746-755. (JOURNAL)
9. Li N, Zeng ZY, Wang Z, Han XH and Chen GM. Experimental study of the energy separation in a vortex tube. International journal of refrigeration. 2015; 55, pp.93-101. (JOURNAL)
10. Dyck NJ, Parker MJ and Straatman AG. The impact of boundary treatment and turbulence model on CFD simulations of the Ranque-Hilsch vortex tube. International Journal of Refrigeration. 2022; 141, pp.158-172. (JOURNAL)
11. Rajpal R, Dhopavkar UH and Lam PAK. Effect of right-angled ribbed geometry on the performance of a Ranque–Hilsch vortex tube: A numerical study. International Journal of Refrigeration. 2023; 151, pp.385-396. (JOURNAL)
12. Singh RK, Pramanick AK and Rana SC. Computational study of temperature separation for a three-dimensional vortex tube with cold exit diameter and nozzle number variation. International Journal of Ambient Energy. 2022; 43(1), pp.7046-7060. (JOURNAL)
13. Singh RK, Pramanick AK and Rana SC. Computational analysis for temperature separation and correlations prediction for dual-inlet-sections vortex tube. Numerical Heat Transfer, Part B: Fundamentals. 2023; 84(4), pp.465-485. (JOURNAL)
14. Singh RK, Pramanick AK and Rana SC. Numerical analysis of temperature separation and exergy analysis of a dual-inlet section convergent vortex tube. Journal of Thermal Science and Engineering Applications. 2023; 15(7), p.071007. (JOURNAL)
15. Singh RK, Pramanick AK, and Rana SC. Computational study for the optimization of Ranque-Hilsch vortex tube with the variation of number of inlet chamber and distance between the chambers. International Symposium on Fluids and Thermal Engineering (FLUTE 2021); 22 July 2021; Uttar Pradesh, India: IOP Publishing. Journal of Physics: Conference Series; 2022.Vol. 2178, No. 1, p. 012010). (CONFERENCE PROCEEDINGS)
16. Singh RK, Pramanick AK and Rana SC. Computational study of the effect of cold orifice dimension on the temperature variation in the counter flow vortex tube. 2nd International Conference on Future Learning Aspects of Mechanical Engineering; 5 Aug 2020; Amity University Noida, India: Springer Singapore; Advances in Fluid and Thermal Engineering: 2022; pp. 313-325. (CONFERENCE PROCEEDINGS)

17. Singh RK, Pramanick AK and Rana SC. Computational study for the cooling performance and effect of insulation on the vortex tube with different insulating material. Numerical Heat Transfer, Part A: Applications. 2023; pp.1-19. (JOURNAL)
18. Singh RK, Pramanick AK and Rana SC. Numerical study of a double inlet chamber counter flow vortex tube with insulation. Second International Conference on Sustainable Energy Solutions for a Better Tomorrow (SESBT 2021) 23rd-24th July 2021, Vellore Institute of Technology (VIT) Chennai, Tamilnadu, India. In IOP Conference Series: Earth and Environmental Science: 2021; Vol. 850, No. 1, p. 012024. (CONFERENCE PROCEEDINGS)
19. Singh RK, Mahato SK, Pramanick AK and Rana SC. Numerical analysis for the thermal performance and flow separation in the vortex tube with different design of flow control valve. Journal of the Brazilian Society of Mechanical Sciences and Engineering. 2024; 46(2), p.88. (JOURNAL)
20. Singh RK, Mahato A, Pramanick AK and Rana SC. Study of the Impact of Flow Valve Design on the Temperature Separation in the Vortex Tube with Computational Approach. Fluid Mechanics and Fluid Power, IIT Roorkee, 14th dec 2022; Springer Nature Singapore: 2024; pp. 643-656). (CONFERENCE PROCEEDINGS)
21. Singh RK, AK Pramanick, and SC Rana. Investigation of counter flow vortex tube with insulation and its effects on the thermal performance using a computational fluid dynamic approach. 26thNational and 4th International ISHMT-ASTFE Heat and Mass Transfer Conference December 17-20, 2021, IIT Madras, Chennai-600036, Tamil Nadu, India. Begel House Inc., 2021. (CONFERENCE PROCEEDINGS)
22. Thakare HR, Parekh AD. Experimental investigation & CFD analysis of Ranque–Hilsch vortex tube. Energy. 2017; 133:284– 298. (JOURNAL)

